Supporting Information

for

Design Guidelines to Elongate Spin−Lattice Relaxation Time of Porphyrins with Large Triplet Electron Polarization

Akio Yamauchi,[†,§] Saiya Fujiwara,[†,§] Koki Nishimura,[†] Yoichi Sasaki,[†] Kenichiro Tateishi,[,‡] Tomohiro Uesaka,[‡]   Nobuo Kimizuka,[*,†] and Nobuhiro Yanai[*,†,#]*

[†]Department of Chemistry and Biochemistry, Graduate School of Engineering, Center for Molecular Systems (CMS), Kyushu University, 744 Moto-oka, Nishi-ku, Fukuoka 819-0395, Japan
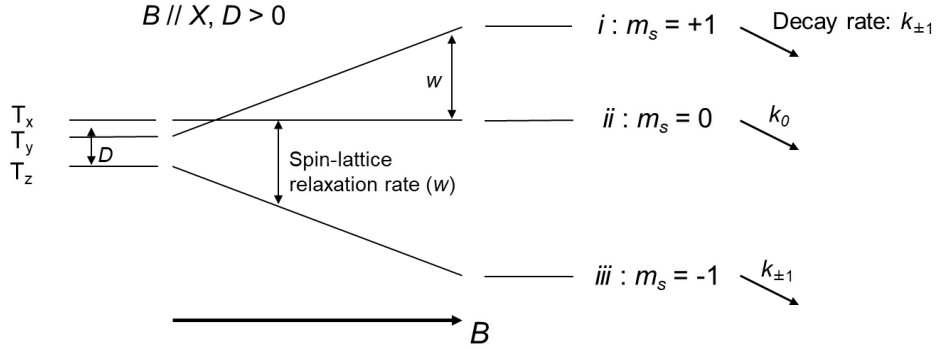
[‡]Cluster for Pioneering Research, RIKEN, RIKEN Nishina Center for Accelerator-Based Science, 2-1 Hirosawa, Wako, Saitama 351-0198, Japan

[#]JST-PRESTO, Honcho 4-1-8, Kawaguchi, Saitama 332-0012, Japan

Brief summary of the deviation of equation (1)

The derivation of the equation (1) can be found in a recent paper by Matsuoka et al.[1] and is briefly summarized here. The spin dynamics is assumed as Scheme S1.

Scheme S1. Schematic Diagram of the spin dynamics of the triplet electron in the magnetic field

Under the high field approximation, the decay rate from the higher and lower spin sublevels becomes equal ($k_+ = k_-$). The population of the higher and lower triplet sublevels becomes equal in high field ($P_+ = P_-$). In the high temperature limit, the rate of spin−lattice relaxation from the lower to higher spin sublevels is assumed to be the same as that of the opposite transition ($w = w_{ij} = w_{ji}$). In case of porphyrins, the spin−lattice relaxation ($\sim \mu$s) is much faster than the decay from the triplet state to the singlet ground state ($\sim$ ms), *i.e.* $w \gg \Delta k$, k_{av}.

Under the high field, the change of the populations expressed by following differential equation.

$$\frac{d\boldsymbol{P}}{dt} = -\boldsymbol{KP} - \boldsymbol{WP}$$

The population $\boldsymbol{P}$ of the triplet sublevels P_{+1}, P_0 and P_{-1} in high field is given by

$$\boldsymbol{P} = \begin{pmatrix} P_{\pm 1} \\ P_0 \\ P_{\pm 1} \end{pmatrix}$$

The matrix $\boldsymbol{K}$ is expressed by anisotropy of the decay rates ($k_{\pm}$ and k_0) from the triplet state to the singlet ground state as

$$K = \begin{pmatrix} k_{\pm 1} & 0 & 0 \\ 0 & k_0 & 0 \\ 0 & 0 & k_{\pm 1} \end{pmatrix}$$

The matrix W is given using the spin−lattice relaxation rate w as

$$W = \begin{pmatrix} w & -w & 0 \\ -w & 2w & -w \\ 0 & -w & w \end{pmatrix}$$

The differential equation is written as follows:

$$\frac{d}{dt}\begin{pmatrix} P_{\pm 1} \\ P_0 \end{pmatrix} = \begin{pmatrix} -(w + k_{\pm 1}) & w \\ 2w & -(2w + k_0) \end{pmatrix} \begin{pmatrix} P_{\pm 1} \\ P_0 \end{pmatrix}$$
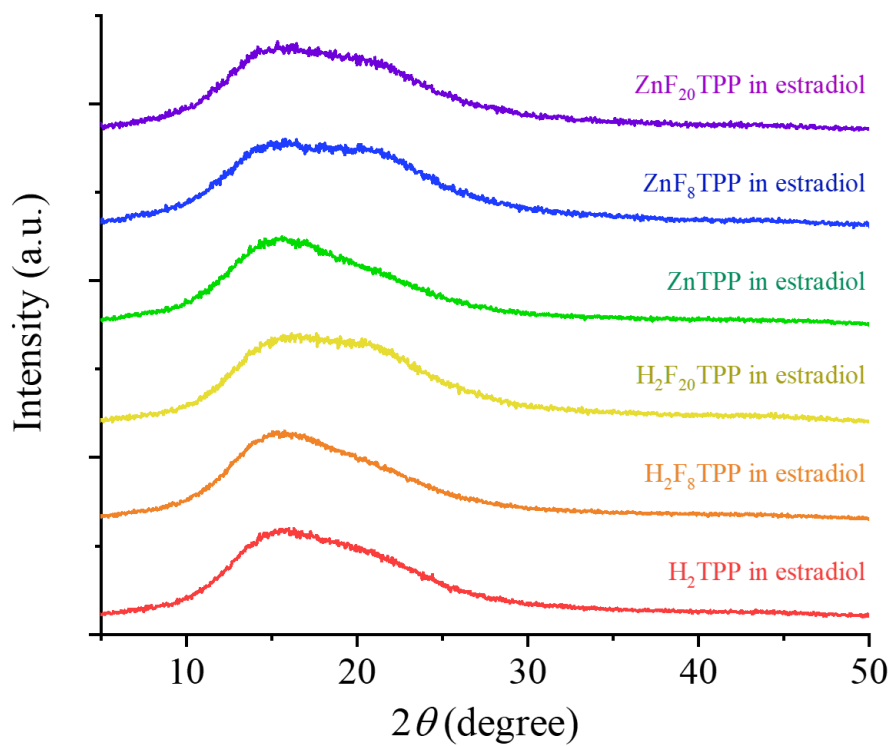
Under the condition of fast relaxation ($w \gg \Delta k, k_{av}$), This equation can be solved as follows:

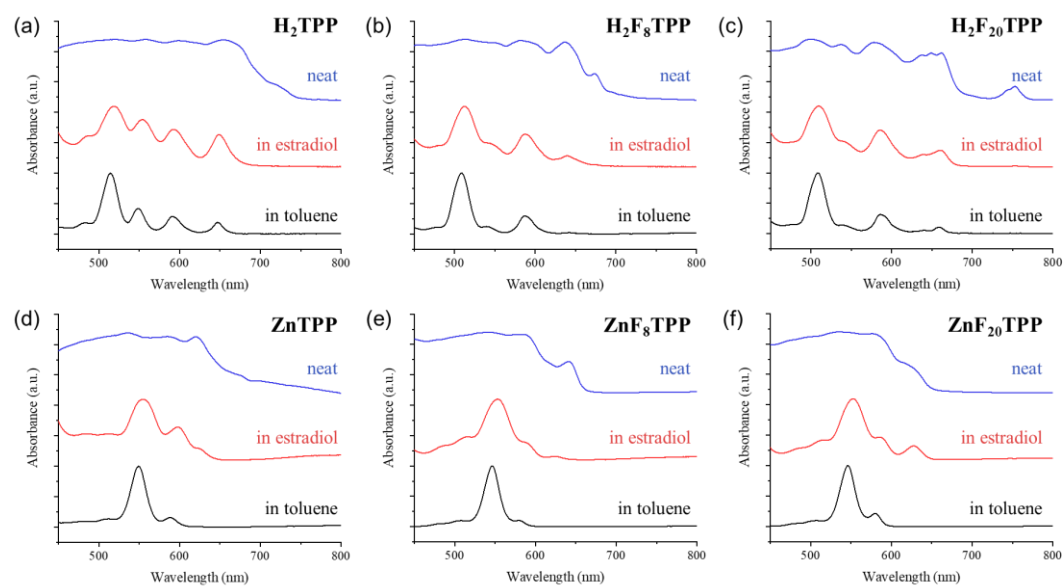$$P_\Delta = \pm(P_0 - P_{\pm 1})\exp\{-(3w + k_{av})t\}$$

The decay constant of this equation can be divided into the spin−lattice relaxation term and the triplet decay term, so it can be transformed by taking the inverse of each term as follows

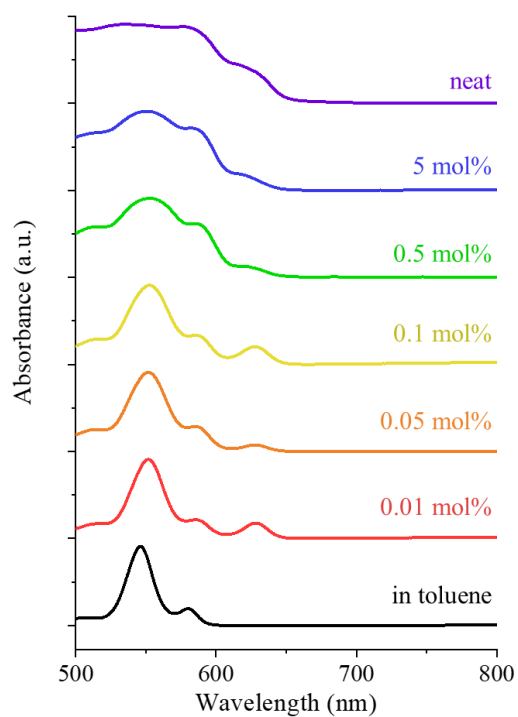$$P_\Delta = \pm(P_0 - P_{\pm 1})\exp\{-(1/T_1 + 1/T_{tri})t\}$$

where T_1 and T_{tri} are the spin−lattice relaxation time and triplet lifetime, respectively.
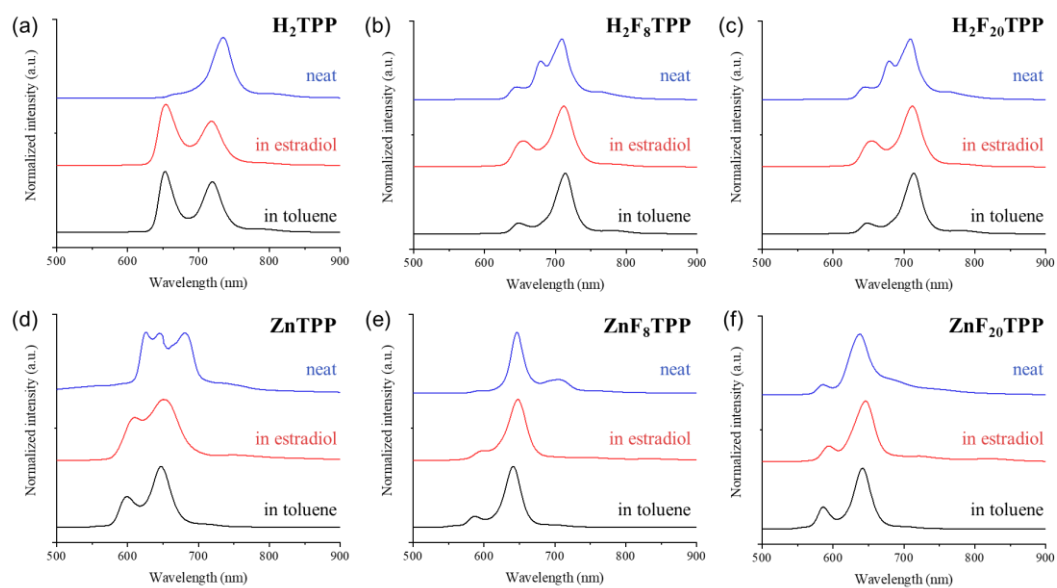
Figure S1. PXRD patterns of β-estradiol glass doped with 0.1 mol% H_2TPP (red), H_2F_8TPP (orange), $H_2F_{20}TPP$ (yellow), ZnTPP (green), ZnF_8TPP (blue) and $ZnF_{20}TPP$ (purple).

Figure S2. UV−vis absorption spectra of (a) H_2TPP, (b) H_2F_8TPP, (c) $H_2F_{20}TPP$, (d) ZnTPP, (e) ZnF_8TPP and (f) $ZnF_{20}TPP$ in toluene (20 µM, black line) in β-estradiol glass (0.1 mol%, red line) and neat solid (blue line).

Figure S3. Absorption spectra of ZnF$_{20}$TPP in toluene (20 µM, black line), ZnF$_{20}$TPP in *β*-estradiol glass at concentrations of 0.01 mol% (red), 0.05 mol% (orange), 0.1 mol% (yellow), 0.5 mol% (green) and 5 mol% (blue), and ZnF$_{20}$TPP neat solid (purple).
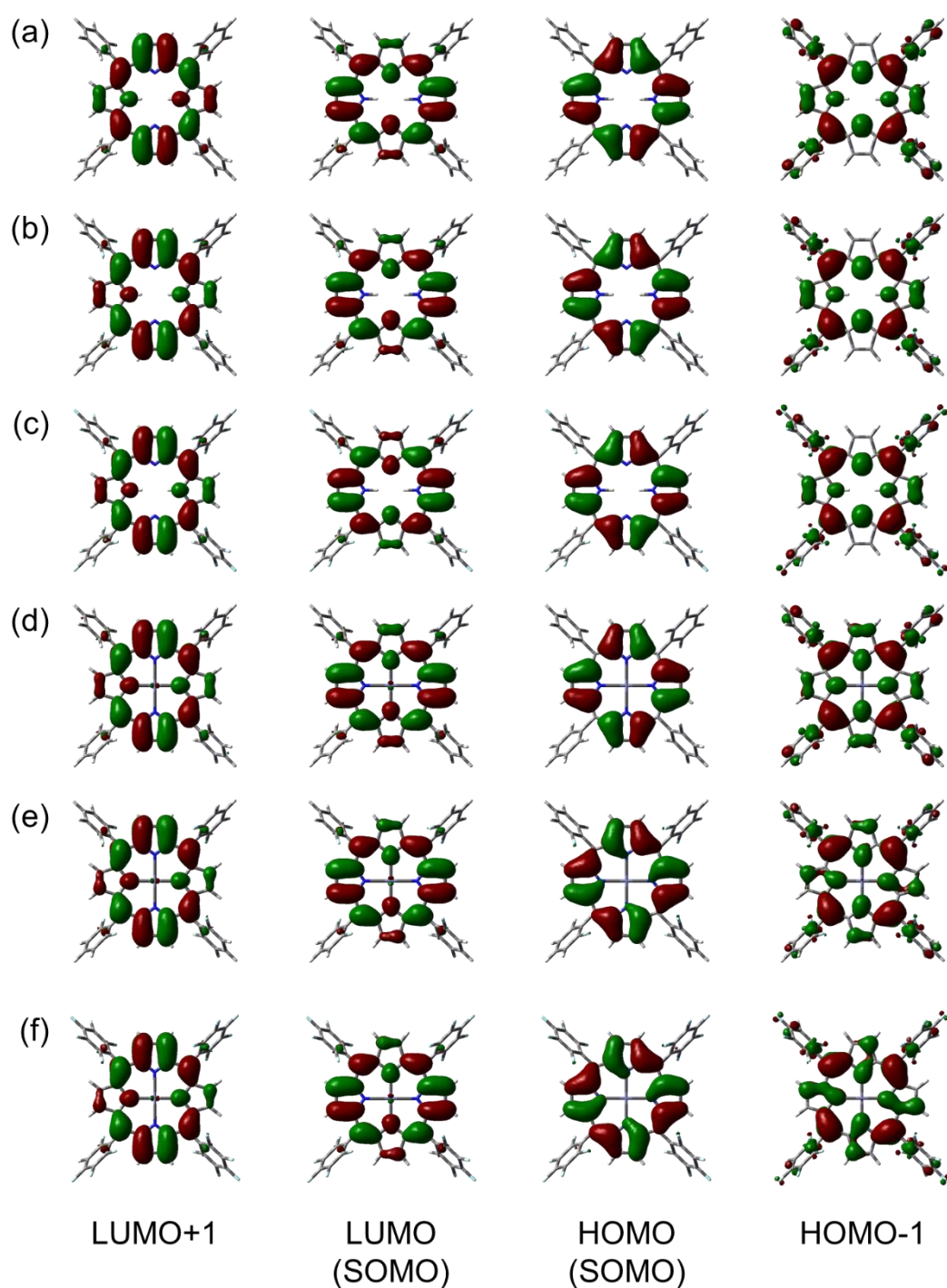
Figure S4. Fluorescence spectra of (a) H_2TPP, (b) H_2F_8TPP, (c) $H_2F_{20}TPP$, (d) ZnTPP, (e) ZnF_8TPP and (f) $ZnF_{20}TPP$ in toluene (20 μM, black line), in β-estradiol glass (0.1 mol%, red line) and neat solid (blue line). Excitation wavelength was 400-420 nm.

Figure S5. Transient absorption decays (black lines) of (a) H_2TPP (λ_{ex} = 515 nm, λ_{em} = 490 nm), (b) H_2F_8TPP (λ_{ex} = 515 nm, λ_{em} = 450 nm), (c) $H_2F_{20}TPP$ (λ_{ex} = 515 nm, λ_{em} = 460 nm), (d) ZnTPP (λ_{ex} = 550 nm, λ_{em} = 510 nm), (e) ZnF_8TPP (λ_{ex} = 550 nm, λ_{em} = 510 nm) and (f) $ZnF_{20}TPP$ (λ_{ex} = 550 nm, λ_{em} = 510 nm) in β-estradiol glass (0.1 mol%). The results of single exponential fittings are shown as red lines.

LUMO+1	LUMO (SOMO)	HOMO (SOMO)	HOMO-1

Figure S6. The four frontier orbitals (isovalue = 0.02) of (a) H_2TPP, (b) H_2F_8TPP, (c) $H_2F_{20}TPP$, (d) ZnTPP, (e) ZnF_8TPP and (f) $ZnF_{20}TPP$ in the lowest triplet state calculated by B3LYP/6-31G*.

Table S1. Peak positions of UV−vis absorption, fluorescence and phosphorescence spectra of the porphyrins shown in Figure 2.

Compound	Absorption (nm)	Fluorescence (nm)	Phosphorescence (nm)
H_2TPP	514, 549, 591, 647	653, 721	853, 969
H_2F_8TPP	509, 542, 587, 641	650, 714	830, 940
$H_2F_{20}TPP$	508, 543, 586, 640, 659	644, 662, 713	821, 930
$ZnTPP$	549, 588	599, 647	789, 889
ZnF_8TPP	547, 581	586, 641	727, 810
$ZnF_{20}TPP$	546, 580	586, 642	735, 821

Table S2. The excitation energies and main configurations (weight) of the porphyrins in the lowest triplet state calculated with B3LYP/SDD for Zn, EPR-II for others.

Compound	Excitation energy (eV)	HOMO →LUMO	HOMO →LUMO+1	HOMO-1 →LUMO	HOMO-1 →LUMO+1
H_2TPP	1.366	0.830	-	-	0.148
H_2F_8TPP	1.393	0.761	-	-	0.219
$H_2F_{20}TPP$	1.412	0.726	-	-	0.254
ZnTPP	1.649	0.421	0.421	0.075	0.075
ZnF_8TPP	1.684	0.167	0.167	0.328	0.328
$ZnF_{20}TPP$	1.695	0.220	0.220	0.272	0.272

Table S3. Spin density of the porphyrins in the lowest triplet state calculated with B3LYP/6-31G*.

Compound	Porphyrin ring	Phenyl ring	Zn atom
H_2TPP	1.9901	0.0099	-
H_2F_8TPP	1.9987	0.0013	-
$H_2F_{20}TPP$	1.9980	0.0020	-
ZnTPP	1.9739	0.0125	0.0136
ZnF_8TPP	1.9785	0.0122	0.0093
$ZnF_{20}TPP$	1.9896	0.0136	-0.0031

Rerefences

(1) Matsuoka, H.; Retegan, M.; Schmitt, L.; Höger, S.; Neese, F.; Schiemann, O. Time-Resolved Electron Paramagnetic Resonance and Theoretical Investigations of Metal-Free Room-Temperature Triplet Emitters. *J. Am. Chem. Soc.* **2017,** *139*, 12968-12975.